Intramolecular C(sp^3)—H amination of arylsulfonyl azides with engineered and artificial myoglobin-based catalysts

Melanie Bordeaux, Ritesh Singh, Rudi Fasan *

Department of Chemistry, University of Rochester, Rochester, NY 14627, United States

ABSTRACT

The direct conversion of aliphatic C—H bonds into C—N bonds provides an attractive approach to the introduction of nitrogen-containing functionalities in organic molecules. Following the recent discovery that cytochrome P450 enzymes can catalyze the cyclization of arylsulfonyl azide compounds via an intramolecular C(sp^3)—H amination reaction, we have explored here the C—H amination reactivity of other hemoproteins. Various heme-containing proteins, and in particular myoglobin and horseradish peroxidase, were found to be capable of catalyzing this transformation. Based on this finding, a series of engineered and artificial myoglobin variants containing active site mutations and non-native Mn- and Co-protoporphyrin IX cofactors, respectively, were prepared to investigate the effect of these structural changes on the catalytic activity and selectivity of these catalysts. Our studies showed that metallo-substituted myoglobins constitute viable C—H amination catalysts, revealing a distinctive reactivity trend as compared to synthetic metalloporphyrin counterparts. On the other hand, amino acid substitutions at the level of the heme pocket were found to be beneficial toward improving the stereo- and enantioselectivity of these Mb-catalyzed reactions. Mechanistic studies involving kinetic isotope effect experiments indicate that C—H bond cleavage is implicated in the rate-limiting step of myoglobin-catalyzed amination of arylsulfonyl azides. Altogether, these studies indicate that myoglobin constitutes a promising scaffold for the design and development of C—H amination catalysts.

© 2014 Elsevier Ltd. All rights reserved.

1. Introduction

The abundance of amine-containing functionalities in both natural and synthetic bioactive molecules makes the development of catalytic strategies for the direct amination of C(sp^3)—H bonds a prominent goal in organic synthesis. Over the past decade, significant advances have been made toward the development of transition metal catalysts for catalyzing C—H amination transformations via metal-nitrenoid C—H insertion.[1–3] In this area, notable strategies for intramolecular C—H amination have involved the use of rhodium-based catalysts with in situ-generated iminoiodanes as nitrene sources.[4–6] Catalytic systems based on Ir-,[7,8] Ru-,[9] Ag-,[10] and Fe-complexes[11,12] have also proven useful for promoting intramolecular C(sp^3)—H amination reactions in the presence of iminoiodane reagents. Considerable efforts have also focused on exploring the reactivity of metalloporphyrins (i.e. Fe-, Mn-, Co-, Ru-porphyrins) toward supporting the amination of aliphatic C—H bonds in both intra- and intermolecular settings.[13–17] Whereas initial work in this area

has also involved the use of iminoiodinanes,[13,14,16] an important advancement in the field has involved the extension of the scope of these catalysts, and in particular cobalt-porphyrins (e.g. Co^{II}(TPP); TPP = tetraphenylporphyrin), to organic azides.[15,17,18] Organic azides indeed represent practically convenient and atom-economical nitrene sources for amination reactions, as nitrogen is typically released as the only by-product of the reaction.

While the aforementioned studies have focused synthetic catalysts for C—H amination reactions, our group and others have recently demonstrated that engineered cytochrome P450 enzymes with both native[19] and serine-ligated heme[20] can provide viable catalysts for promoting intramolecular C—H amination transformations with arylsulfonyl azide substrates. In particular, our studies evidenced the direct involvement of the P450-embedded heme cofactor, in the reduced, ferrous form, for mediating these reactions. Based on initial experimental data, we proposed a mechanism for these transformations that invokes the formation of an imido-iron(IV)(ppIX) species (ppIX = protoporphyrin IX) followed by metal-nitrenoid insertion into the benzylic C—H to give the corresponding benzosultam product.[19] Altogether, these studies suggested that other heme-dependent enzymes and hemoproteins could potentially exhibit C—H amination reactivity, which

constitutes the focus of the present study. Upon discovery that myoglobin can catalyze this reaction, we further examined the effect of structural modifications, involving both amino acid mutations of the level of heme pocket as well as substitution of the heme with non-native metalloporphyrin cofactors, on the amination activity and stereoselectivity of these myoglobin-based catalysts. In addition, kinetic isotope effect experiments were performed to gain insights into the mechanism of myoglobin-catalyzed C—H amination within this class of organic azides.

2. Results and discussion

2.1. C—H amination activity of different hemoproteins

The recent discovery that P450s can catalyze the cyclization of arylsulfonyl azides prompted us to investigate whether other heme-containing proteins could exhibit C—H amination reactivity on this class of substrates. To this end, we assembled a panel of different heme-dependent enzymes/proteins consisting of bovine catalase (Cat), horseradish peroxidase (HRP), hemoglobin (Hb), and sperm whale myoglobin (Mb). These proteins feature a significantly different heme environment compared to each other and to the previously investigated P450s. In catalase, the proximal heme-coordination ligand is provided by a Tyr residue,[21] while a His proximal ligand is present in HRP,[22] Hb, and Mb.[23,24] Despite sharing a common heme-ligating residue (His), a strong H-bonding interaction with a neighboring Asp residue (D235) imparts considerable anionic character to the proximal His in HRP as compared to the histidinyl-Fe(heme) system in Hb and Mb.[25] Among others, these structural differences are known to play a key role in modulating the reactivity of these heme-containing proteins toward H_2O_2 dismutation (Cat), H_2O_2 activation (HRP), or molecular oxygen binding (Hb, Mb).[26]

As a model reaction, the cyclization of 2,4,6-triisopropylbenzene-sulfonyl azide (**1**, Fig. 1) was initially utilized to probe the ability of these hemoproteins to catalyze the intramolecular C—H amination of this class of organic azides. Notably, successful conversion of **1** to the corresponding benzosultam product, **4**, was observed in each case under anaerobic conditions and in the presence of sodium dithionite ($Na_2S_2O_4$) as reductant (Fig. 1). These experiments also evidenced the different reactivity of the
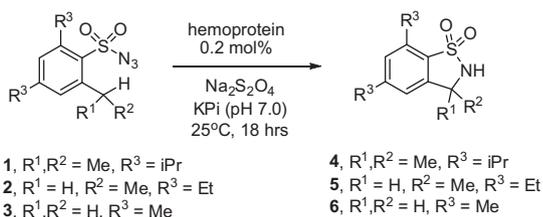
hemoproteins toward the transformation of **1**. In particular, Mb and HRP exhibited the most prominent C—H amination activity, supporting 200–300 total turnovers as compared to <15 for free hemin. In comparison, Hb and Cat showed a 5- to 10-fold lower efficiency under identical reaction conditions. The C—H amination activity of native Mb and HRP on **1** was also found to be considerably higher (10- to 15-fold, respectively) than that of wild-type CYP102A1 (P450$_{BM3}$) investigated previously (20 TTN).[19] Analysis of the turnover frequency (TOF) also showed that Mb and HRP are considerably faster C—H amination catalysts than Hb and Cat (105–120 turnovers h^{-1} vs <50 turnovers h^{-1}, Fig. 1).

As noted in the context of our studies with P450s,[19] the addition of the reductant dithionite was critical for observing C—H amination activity in the above reactions, clearly indicating that the ferrous state is the catalytically active form of these hemoproteins. This is also true for catalase, which unlike HRP, Mb and Hb, cannot be quantitatively converted to the ferrous form by dithionite as determined by UV–vis spectroscopy (data not shown). This phenomenon is likely a result of the much lower redox potential of the phenolate-bound heme in catalase ($E^{\circ\prime}$ = −500 mV vs NHE)[27] as compared to the histidinyl-coordinated heme in HRP and Mb ($E^{\circ\prime}$ = −250 and +50 mV vs NHE, respectively).[28,29] This notwithstanding, the lack of product formation in dithionite-free reactions with catalase indicated that a certain amount of the catalytically active ferrous species is generated in the presence of reductant, although the lower propensity toward reduction is likely to be at least in part responsible for the lower C—H amination activity observed for this enzyme as compared to the other hemoproteins.

To explore the substrate scope of these catalysts, we then extended our activity studies to 2,4,6-triethylbenzene-sulfonyl azide (**2**) and 2,4,6-trimethylbenzene-sulfonyl azide (**3**). These compounds contain a II° and I° benzylic C—H bond, respectively, as opposed to the III° benzylic C—H bond in **1**. Overall, much lower TTN values were observed in these reactions (Fig. 1), with the decrease in activity correlating with the increasing strength of the benzylic C—H bond going from **1** to **2** to **3**. Nevertheless, Mb and HRP emerged as the most active C—H amination catalysts also in the context of these less activated substrates. Collectively, these results demonstrated that all the tested hemoproteins can activate the arylsulfonyl azides **1**–**3** in a productive intramolecular C—H amination process, also highlighting the impact of the different heme environment on affecting such reactivity. On the basis of these initial results, Mb was selected for further investigation. Indeed, across the heme-containing enzymes tested, Mb showed the highest C—H amination activity, second only to HRP. This choice was further motivated by the small size (17 kDa), high thermostability (T_m = 82 °C),[30] and ease of expression in *Escherichia coli* of Mb, making this hemoprotein an attractive scaffold for manipulation and thus further optimization.

2.2. Mb active site variants

The inherently chiral active site provided by the protein matrix holds promise toward enabling these biocatalytic C—H amination transformations to proceed in an enantio- or stereoselective manner.[19] Interestingly, analysis of the enantiomeric excess produced in the cyclization of the prochiral substrate **2** catalyzed by wild-type Mb showed the absence of any asymmetric induction (Fig. 2). To examine the enantioselectivity of this hemoprotein, the racemic substrate **8** was also tested. Also in this case, no enantiomeric excess in the formation of the corresponding C—H amination product, **9**, was observed. In contrast, a moderate degree of stereo- and enantioselectivity was measured in the conversion of both **2** and **8** catalyzed by HRP and catalase (Fig. 2). These results prompted us to explore the possibility to improve the stereo- and enantioselectivity of Mb by means of active site mutagenesis.

1, R^1,R^2 = Me, R^3 = iPr
2, R^1 = H, R^2 = Me, R^3 = Et
3, R^1,R^2 = H, R^3 = Me

4, R^1,R^2 = Me, R^3 = iPr
5, R^1 = H, R^2 = Me, R^3 = Et
6, R^1,R^2 = H, R^3 = Me

Catalyst[a]	Product	TTN[b]	TOF[c]	Product	TTN[b]	Product	TTN[b]
Hemin	**4**	12	n.d.	**5**	2	**6**	0
Cat	**4**	56	0.2	**5**	3	**6**	0.1
HRP	**4**	311	121	**5**	12	**6**	0.3
Mb	**4**	181	104	**5**	9	**6**	1
Hb	**4**	27	48	**5**	1	**6**	0

[a] Cat: bovine catalase; HRP: horseradish peroxidase; Mb: sperm whale myoglobin; Hb = human hemoglobin.
[b] Reactions conditions: 20 μM P450, 10 mM azide, 10 mM $Na_2S_2O_4$. Total turnover numbers (TTN) were measured by HPLC from duplicate experiments (SD < 20%).
[c] TOF = turnover frequency expressed in turnovers per hour. N.d. = not determined.

**Figure 1.** C—H amination activity of the hemoproteins on 2,4,6-trialkyl-benzene-sulfonyl azides.
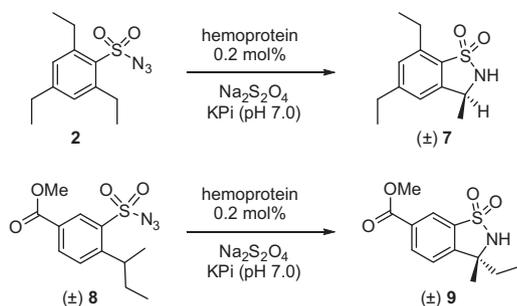
| Catalyst	Product	ee [%][a]	Product	ee [%][a]
Hemin	**7**	0	**9**	0
Cat	**7**	2	**9**	-32
HRP	**7**	12	**9**	-42
Mb	**7**	0	**9**	0
Mb(L29A)	**7**	-16	**9**	-4
Mb(H64V)	**7**	-2	**9**	-36
Mb(V68A)	**7**	14	**9**	-20
Mb(H64V, V68A)	**7**	60	**9**	-2
Mb(L29A, H64V)	**7**	8	**9**	14

[a] Determined by SFC (supercritical fluid chromatography) analysis using authentic racemic standards as reference. Sign indicates whether one or the opposite enantiomer (neg. sign) is formed.

Figure 2. Stereo- and enantioselectivity in the cyclization of **2** and **8** catalyzed by the hemoproteins and the Mb variants.[a]

To this end, a panel of Mb variants were prepared by introducing single (i.e., L29A, H64V, and V68A) and double amino acid substitutions (i.e. L29A/H64V, H64V/V68A) into the active site of the hemoprotein. These mutations affect amino acid residues that protrude into the distal cavity of Mb (Fig. 3), thereby potentially altering the stereo- and enantioselectivity of the hemoprotein in the ring closure of **2** and **8**, respectively. The Mb variants were expressed in *E. coli* and purified via Ni-affinity chromatography. All the proteins were determined to be properly folded as judged based on the characteristic Soret band in their respective electron adsorption spectra (λ_{max} between 408 and 415 nm; cp. λ_{max} = 410 nm for ferric wt Mb). To examine the effect of the mutations on C—H amination activity, the Mb variants were then tested against substrate **1**. These experiments showed that all the proteins exhibited high C—H amination activity, supporting total turnover numbers ranging from 90 to 200 (Fig. 4). Interestingly, a slight
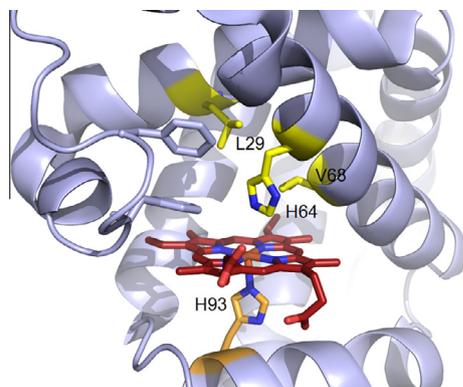
Figure 3. View of the active site of sperm whale myoglobin (pdb 1A6K). The heme and heme-bound 'proximal' His residue (His93) are displayed in red and orange, respectively. The active site residues targeted for mutagenesis are highlighted in yellow.
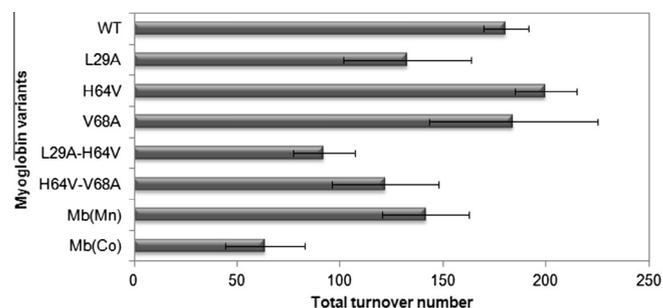
Figure 4. Total turnover numbers of the engineered Mb variants in the C—H amination of 2,4,6-triisopropylbenzene-sulfonyl azide (**1**) under standard reaction conditions. Wild-type Mb is included for comparison.

increase in TTN as compared to wild-type Mb was observed as a result of the H64V mutation. This position corresponds to the 'distal histidine' residue (Fig. 3), which is involved in H-bonding the heme-bound water molecule and molecular oxygen in deoxy-Mb and oxy-Mb, respectively.[23,24] Its substitution with valine could make the heme center more accessible to the substrate, possibly contributing to the observed increase in activity. The effect of this mutation does not appear to be general though, as suggested by the lower TTN values for the double mutant Mb variants, which also contain this mutation (Fig. 4).

Gratifyingly, analysis of the reactions with **2** and **8** indicated a significant effect of the active site mutations on the stereo- and enantioselectivity of the hemoprotein. In the presence of the pro-chiral azide **2**, the largest asymmetric induction was obtained with the double mutant Mb(H64V, V68A) (60% ee vs 0% ee for wt Mb) (Fig. 2). Interestingly, the single mutant Mb(L29A) showed preference for the formation of the opposite enantiomer (16% ee). With the racemic substrate **8**, Mb(H64V) exhibited the largest increase in enantioselectivity as compared to the parent protein (0 → 36% ee), whereas the double mutant Mb(L29A, H64V) produced the opposite enantiomer in larger excess (14% ee) (Fig. 2). In both cases, the effects of the mutations were not found to be additive as judged by comparison of the % ee values across the series of engineered Mb variants. More importantly, these studies showed that the stereo- and enantioselectivity of the Mb-based C—H amination catalysts toward either enantiomeric product could be modulated and, to a certain extent, improved by protein engineering.

2.3. ChuA-based system for recombinant expression of metallo-substituted Mb variants

Zhang and coworkers recently reported that synthetic metalloporphyrins such as Co-, Fe-, and Mn-tetraphenylporphyrins (TPPs) can also catalyze the intramolecular C—H amination of arylsulfonyl azides, supporting about 40–50 turnovers under optimized conditions.[17] Interestingly, these studies showed a large dependence of the catalytic activity on the nature of the metal center. In particular, the following order of reactivity was found: Co(TPP) >> Fe(TPP) > Mn(TPP) as indicated by the respective number of turnovers (~50, 5, and 2, respectively) observed in the presence of 2,4,6,triisopropylbenzene sulfonyl azide (**1**) in chlorobenzene.[17] These observations raised the intriguing question of whether similar effects on C—H amination reactivity would be observed upon substitution of the metal center in the Mb-based catalysts investigated here.

Mn- and Co-substituted Mb variants have been previously obtained by reconstitution of apoMb with the corresponding metallo-protoporphyrins IX.[31–33] This approach however involves laborious and time-consuming refolding and purification procedures. Inspired by recent work in the context of

metallo-substituted P450s,[34] we sought to implement a convenient and practical strategy for the recombinant expression of metallo-substituted Mb variants by utilizing *E. coli* cells co-expressing an heterologous, outer-membrane heme transporter (ChuA).[35] Accordingly, wild-type Mb and the heme transporter ChuA from O157:H7 *E. coli*[35] were initially expressed in BL21(DE3) cells using a dual plasmid system in which the Mb and ChuA genes were placed under an IPTG-inducible promoter. Cells were grown in M9 minimal medium supplemented with Mn^{III}(ppIX). Under these conditions, Mn-substituted Mb (Mb(Mn^{III})) could be successfully isolated with a yield of approximately 5 mg/L of culture. In order to increase the expression yield, further optimization of the system was then carried out by varying the ChuA-containing plasmid constructs, energy source (glucose vs glycerol), and the concentration of Mn^{III}(ppIX) in the medium. The most representative results from these experiments are summarized in Table 1.

Upon observation that a good fraction of the expressed Mb accumulated in the form of inclusion bodies, a second plasmid encoding for both ChuA and the chaperone complex, GroEL/ES, was prepared. The latter was expected to increase the fraction of the desired protein in correctly folded and soluble form. Gratifyingly, this system led to a significant increase (2.5-fold) in the yield of Mb(Mn^{III}) (13 vs 5 mg/L culture). This improvement was however accompanied by a reduction in the fraction of Mb(Mn^{III}) in the total isolated Mb (100 → 70%, the remainder being wild-type Mb) as quantified by electron absorption spectroscopy (vide infra). Under further optimized conditions (glycerol as energy source and Mn(ppIX) at 30 µg/mL), the expression yield could be raised to 19 mg/L culture with quantitative incorporation of Mn^{III}(ppIX). Finally, a further 25% increase in the yield of Mb(Mn^{III}) was obtained by using C41(DE3) cells as the expression host. This *E. coli* strain is an engineered derivative of BL21(DE3) which favors the expression of toxic proteins.[36] This choice was based on the observed reduction in cell viability as a result of the co-expression of the membrane protein ChuA as determined in control experiments. Overall, a 500% increase in the isolated yield of the desired Mb(Mn^{III}) variant was achieved as compared to the initial system (Table 1). This protocol could be then applied for the expression and isolation of Mb(Co^{III}) in good yield (16 mg/L culture).

2.4. Spectroscopic characterization and C—H amination activity of Mn- and Co-containing Mb catalysts

The purified Mb(Mn) and Mb(Co) variants were characterized by electron absorption spectroscopy in both oxidized and reduced form. As shown in Figure 5B, Mb(Mn^{III}) shows a split Soret band with λ_{max} at 375 and 469 nm in phosphate buffer at pH 7.0. Upon addition of dithionite, a single Soret band with λ_{max} at 438 nm becomes apparent, indicating complete reduction of the protein to Mb(Mn^{II}). On the other hand, the visible spectrum of Mb(Co^{III}) shows a prominent absorption band at 422, which shifts to 401 nm under reducing conditions, thus evidencing the formation
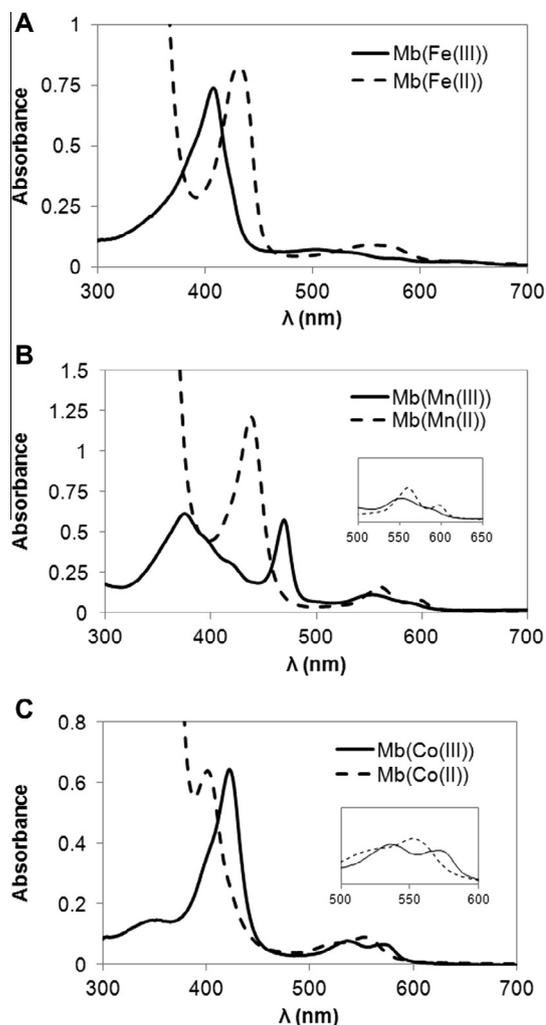
Figure 5. Metallo-substituted Mb variants. Overlay plot of the electronic absorption spectrum of (A) wild-type Mb, (B) the Mn-containing Mb variant, and (C) Co-containing Mb variant, in oxidized (solid line) and reduced form (dotted line). The Q band regions are enlarged in the inserts.

of the reduced form, Mb(Co^{II}) (Fig. 5C). These spectroscopic features are consistent with those reported for Mn- and Co-containing myoglobins prepared by other methods.[33]

To examine the effect of metal substitution on the C—H amination reactivity of Mb, reactions were carried out using substrate **1** and the Mn- and Co-containing Mb variants. Interestingly, these studies showed that both of the metallo-substituted Mb possess C—H amination activity (Fig. 4). As for wild-type Mb, formation of the benzosultam product **4** was observed only when dithionite was added to reaction mixture, clearly indicating that Mb(Mn^{II})

Table 1
Optimization of expression conditions for production of Mn-substituted myoglobin (=Mb(Mn^{III}))

Entry	Expression system[a]	Bacterial strain	Carbon source	[Mn^{III}(ppIX)] (mg/L culture)	Mb(Mn^{III}) yield (mg/L culture)	% Mb(Mn)[b]
1	ChuA (*lacUV5*)	BL21(DE3)	Glycerol	30	5	100
2	ChuA(*T7*) + GroEL/ES(*ara*)	BL21(DE3)	Glucose	30	14	70
3	ChuA(*T7*) + GroEL/ES(*ara*)	BL21(DE3)	Glycerol	0	0	0[c]
4	ChuA(*T7*) + GroEL/ES(*ara*)	BL21(DE3)	Glycerol	6	13	59
5	ChuA(*T7*) + GroEL/ES(*ara*)	BL21(DE3)	Glycerol	30	19	100
6	ChuA(*T7*) + GroEL/ES(*ara*)	C41(DE3)	Glycerol	30	23	100

[a] Co-expressed protein (promoter).
[b] Relative to total amount of Mb expressed. When <100%, the remainder is wt Mb.
[c] Only wild-type Mb (8 mg/L culture).
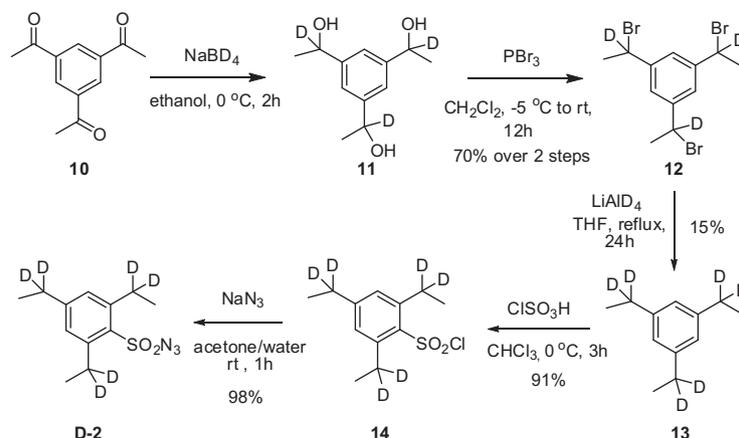
Scheme 1. Synthesis of the deuterated probe substrate **D-2**.

and Mb(Co^{II}) are catalytically active unlike their respective counterparts at the higher oxidation state. Notably, Mb(Mn^{II}) was found to support nearly as many total turnovers as Mb (142 vs 181 TTN, Fig. 4). In contrast, Mb(Co^{II}) was determined to be a considerably less efficient C—H amination catalyst (64 TTN). The impact of metal substitution in these catalysts was also evident from comparison of the respective turnover rates. Indeed, both Mb(Mn^{II}) and Mb(Co^{II}) convert **1** at a significantly slower rate (10-fold) than Mb (9 and 4 turnovers h^{-1} vs 104 turnovers h^{-1}, respectively). In each case, the large activity enhancement resulting from having the metalloporphyrin cofactor embedded in the protein scaffold as opposed to free in solution was evident from the much lower TTN obtained in the presence of substrate **1** with either free Mn^{II}(ppIX) (TTN: 11) or Co^{II}(ppIX) (TTN: 5).

In light of these data, it is interesting to compare the reactivity of these metallo-substituted Mb-based catalysts with that of synthetic metalloporphyrins.[17] A first striking difference concerns the fact that whereas Mb and Mb(Mn) exhibit C—H amination activity only in the reduced form, the corresponding metallotetraphenylporphyrin complexes (i.e. Fe^{III}(TPP) and Mn^{III}(TPP)) are active at the higher oxidation state. This is not the case for Mb(Co^{II}) and Co^{II}-TPP though, which are both active toward these C—H amination reactions. Furthermore, the order of reactivity exhibited by the Mb-based catalysts (Mb > Mb(Mn) >> Mb(Co), Fig. 4) is almost completely reversed compared to the synthetic metalloporphyrin systems (Co^{II}(TPP) >> Fe^{III}(TPP) > Mn^{III}(TPP))[17]. These differences are likely to stem from the combined effect of the different coordination status at the metal center, electronic properties of the porphyrin ring (ppIX vs TPP), and dielectric constant of the porphyrin environment between the two systems. An important conclusion from these studies is the C—H amination reactivity of synthetic porphyrin systems constitutes a poor predictor of that of analogous metalloporphyrin cofactors embedded in the protein scaffold.

2.5. Kinetic isotope effect experiments

Drawing a similarity with the P450 systems investigated previously,[19] we hypothesize that the Mb-catalyzed C—H amination reactions presented here involve the activation of the sulfonyl azide by the ferrous Mb, Mb(Fe^{II}), to give an arylsulfonimido-iron(IV) intermediate ((Mb)Fe^{IV} = NSO$_2$Ar). This reactive species would undergo a nitrene insertion into the benzylic C—H bond of the substrate. Within this mechanism, activation of the C(sp^3)—H bond is expected to be rate limiting, a phenomenon that would be manifested by a positive primary kinetic isotope effect (KIE).
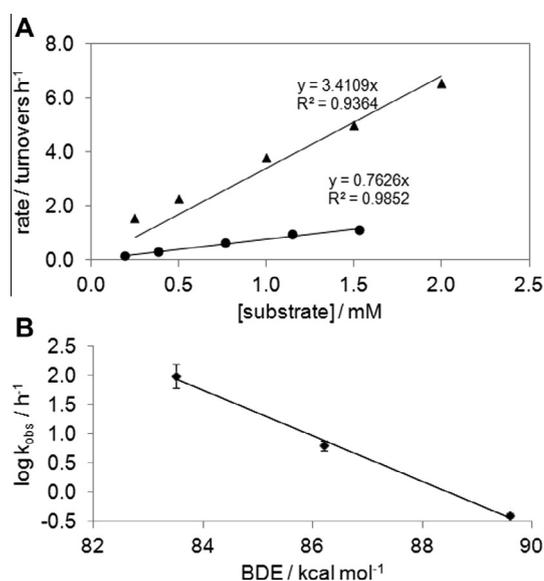
Figure 6. Kinetic analysis and KIE studies. (A) Plots of initial rate versus substrate concentration for Mb-catalyzed amination of substrate **2** (triangles) and its deuterated analog, **D-2** (circles). (B) Plot of logk_{obs} for the Mb-catalyzed amination of substrates **1–3** against the bond dissociation energy (BDE) of the corresponding benzylic C—H bond.

To examine this aspect, a deuterated derivative of compound **2**, **D-2** (Scheme 1) was synthesized. As depicted in Scheme 1 and 1,3,5 triacetyl benzene (**5**) was first reduced with NaBD$_4$ followed by bromination to provide intermediate **7**. Treatment of this compound with LiAlD$_4$ furnished d-6 triethyl benzene **8**. Chlorosulfonation of **8** followed by treatment of the resulting 2,4,6-tri-ethyl-benzene-sulfonyl chloride (**9**) with sodium azide then yielded the target probe compound, **D-2**.

Substrate **2** and its deuterated derivative, **D-2**, were then utilized to measure the KIE (k_H/k_D) resulting from H/D substitution of the benzylic position (Fig. 6A). The KIE value obtained from these experiments was 4.5 ± 0.4 at 20 °C.

In addition, the C—H amination rate of wild-type Mb for the series of structurally related substrates **1–3** was logarithmically plotted against the bond dissociation energy (BDE) of the corresponding benzylic C(sp^3)—H bond. This plot revealed a large and inverse linear relationship between these parameters (Fig. 6B). Altogether, these results are consistent with the hypothesis that activation of the C—H bond is involved in the

rate-determining step of the reaction. Interestingly, the observed KIE value in the Mb reactions is lower than those measured for C—H amination reactions catalyzed by Ru-porphyrin complexes $(k_H/k_D = 6–12)$,[14] but significantly higher than those observed for Rh-complexes $(k_H/k_D = 1.8)$[37] in the presence of structurally related sulfonamide substrates. This difference hints at important differences in the factors affecting the kinetics of Mb-catalyzed amination as compared to these previously investigated systems, which themselves are known to operate via distinct C—H activation pathways (i.e. stepwise vs. concerted nitrene C—H insertion, respectively). Thus, the present data clearly evidence the importance of C—H activation in the Mb-catalyzed amination of arylsulfonyl azides, although future studies are called for to shed further light into the mechanism of these transformations.

3. Conclusions

In summary, this work provides a first demonstration that various heme-containing proteins, and in particular myoglobin and horseradish peroxidase, constitute efficient catalysts for the C—H amination of arylsulfonyl azides. Through the analysis of active site Mb variants, we showed that the limited stereoinduction provided by the native myoglobin scaffold could be addressed via protein engineering, resulting in Mb-based catalysts with improved stereo- and enantioselectivity. To gain facile access to metallo-substituted Mb variants, we have implemented an efficient strategy for the recombinant expression of these artificial Mb catalysts in E. coli which does not require the use of specialized strains.[38] Characterization of the Mn- and Co-substituted Mb revealed intriguing differences with respect to the C—H amination reactivity of these Mb-based catalytic systems as compared to synthetic metalloporphyrins. Finally, our KIE experiments demonstrated the involvement of C—H activation in the rate-determining step of these Mb-catalyzed transformations. We anticipate these studies will provide a basis for the further development and optimization of engineered and artificial Mb-based catalysts for C—H amination reactions.

4. Materials and methods

4.1. Reagents and substrates

All solvents and reagents were purchased from commercial suppliers (Sigma–Aldrich, ACS Scientific, Acros) and used without any further purification, unless stated otherwise. 2,4,6 Tri-isopropylsulfonyl azide (1) was purchased, whereas the other aryl-sulfonyl azides (2, 3, and 8) were synthesized as described previously.[19] Bovine catalase, human hemoglobin, and horseradish peroxidase were purchased from Sigma Aldrich.

4.2. Cloning and mutagenesis of Mb variants

The gene encoding for sperm whale myoglobin was amplified from plasmid pMYO[39] (Addgene plasmid 34626) using primers Myo_NdeI_for and Myo_XhoI_rev (Table S1). The PCR product was cloned into the Nde I/Xho I cassette of plasmid pET22b (Novagen) to give pET22_MYO. The cloning process introduced a His tag at the C-terminus of the protein. The single-mutant Mb variants were prepared by SOE PCR using the corresponding primers provided in Table S1. The double mutants Mb(L29A,H64V) and Mb(H64V,V68A) were obtained in a similar manner by combination of the corresponding mutations.

4.3. Construction of ChuA-containing plasmids

A first pACYC-derived plasmid (pHPEX2)[35] containing E. coli O157:H7 ChuA gene under a lacUV5 promoter was kindly provided

by Professor Douglas Goodwin (Auburn University). A second pACYC-based plasmid (pGroES/EL-ChuA) was constructed by inserting the ChuA gene under a T7 promoter and E. coli GroES/EL gene under an araBAD promoter. To generate this construct, the ChuA gene was amplified from pHPEX2 using primers T7_ChuA_SacI_for and ChuA_XhoI_rev (Table S1) and cloned into a Sac I/Xho I cassette of the pACYC-derived vector. The GroES-EL chaperone genes were amplified from E. coli genomic DNA using primers GroEL/ES_BglII_for and GroEL/ES_SalI_rev (Table S1) and cloned into the Bgl II/Sal I cassette of the same vector.

4.4. Expression and purification of Mb variants

Wild-type Mb and the engineered Mb variants were expressed in E. coli BL21(DE3) cells. Typically, cells were grown in Terrific Broth medium (ampicillin, 100 mg L^{-1}) at 37 °C (150 rpm) until OD$_{600}$ reached 0.6. Cells were then induced with 0.25 mM β-D-1-thiogalactopyranoside (IPTG) and 0.3 mM δ-aminolevulinic acid (ALA). After induction, cultures were shaken at 150 rpm and 27 °C and harvested after 20 h by centrifugation at 4000 rpm at 4 °C. After cell lysis by sonication, the proteins were purified by Ni-affinity chromatography using the following buffers: loading buffer (50 mM Kpi, 800 mM NaCl, pH 7.0), wash buffer 1 (50 mM Kpi, 800 mM NaCl, pH 6.2), wash buffer 2 (50 mM Kpi, 800 mM NaCl, 250 mM glycine, pH 7.0) and elution buffer (50 mM Kpi, 800 mM NaCl, 300 mM L-histidine, pH 7.0). After buffer exchange (50 mM Kpi, pH 7.0), the enzymes were stored at −80 °C. Myoglobin concentration was determined using an extinction coefficient $\varepsilon_{410} = 157$ mM^{-1} cm^{-1}.[40]

4.5. Expression of Co- and Mn-substituted myoglobin

E. coli BL21(DE3) (or C41(DE3) (Lucigen)) cells were co-transformed with the Mb-encoding plasmid (pET22_MYO) and the ChuA-encoding vectors pHPEX2 or pGroES/EL-ChuA. Cells were grown in M9 minimal media supplemented with micronutrients and the appropriate antibiotics at 37 °C until the OD$_{600}$ reached 0.6. Cell cultures were then induced with 0.25 mM β-D-1-thiogalactopyranoside (IPTG) and added with Mn^{III}(ppIX) or Co^{III}(ppIX) to a final concentration of 6 or 30 µg/mL. Cells containing the pGroES/EL-ChuA vector were also induced with 0.5% arabinose at this point. After induction, cultures were shaken at 150 rpm and 27 °C and harvested after 20 h by centrifugation at 4000 rpm at 4 °C. Proteins were purified as described above. Extinction coefficient $\varepsilon_{424} = 152.5$ mM^{-1} cm^{-1} and $\varepsilon_{470} = 60$ mM^{-1}cm^{-1} were used to determine the concentration of Mb(Co^{III}) and Mb(Mn^{III}), respectively.[33] Electronic absorption spectra were recorded in phosphate buffer (50 mM, pH 7.0) at 20 °C.

4.6. C—H amination reactions

Reactions for determination of total turnovers were carried out at a 400 µL scale using 20 µM hemoprotein, 10 mM substrate, and 10 mM sodium dithionite. In a typical procedure, a solution containing sodium dithionate (100 mM stock solution) in potassium phosphate buffer (50 mM, pH 7.0) was degassed by bubbling argon into the mixture for 5 min in a sealed vial. A buffered solution containing the hemoprotein was carefully degassed in a similar manner in a separate vial. The two solutions were then mixed together via cannulation. Reactions were initiated by addition of 8 µL of azide (from a 0.5 M stock solution in methanol) with a syringe, and the reaction mixture was stirred for 18 h at room temperature, under positive argon pressure. Reactions for analysis of C—H amination rates were carried out as described above with the difference that 40 µM hemoprotein was used and that they were stopped after 30 min.

4.7. Product analysis and analytical methods

Reaction mixtures were added with 20 μL of a guaiacol internal standard solution (80 mM in methanol), followed by extraction with 400 μL dichloromethane (DCM). The organic layer was removed via evaporation and the residue was dissolved in 120 μL methanol, followed by HPLC analysis. HPLC analyses were performed on a Shimadzu LC-2010A-HT equipped with a VisionHT C18 column and a UV–vis detector. Injection volume: 10 μL. Flow rate: 1 mL/min. Gradient: 30% acetonitrile in water (0.1% TFA) for 3 min, then increased to 90% over 27 min. Calibration curves for the different sultams were constructed using authentic standard prepared synthetically as previously described.[19] All measurements were performed at least in duplicate. For each experiment, negative control samples containing either no enzyme or no reductant were included. For enantio- and stereoselectivity determination, the samples were analyzed by Supercritical Fluid Chromatography using a JASCO SF-2000 instrument equipped with Chiralpak IA chiral column (4.6 m i.d. × 250 mm) and isocratic elution with CO_2/isopropanol mixture (75:25). Authentic standards of racemic (±)-**7** and (±)-**9** were used for enantiomeric excess determination.

4.8. Synthesis of deuterated probe compound D-2

4.8.1. 1,3,5-Tris(1-bromoethyl-1-*d*)benzene (12)

To a stirred solution of 1,3,5-triacetyl benzene (**10**) (1 g, 4.9 mmol) in ethanol (15 mL) at 0 °C was added NaBD$_4$ (558 mg, 14.7 mmol). Upon completion of the reaction (∼2 h), the reaction mixture was quenched with H_2O (1 mL) followed by extraction with ethyl acetate (3 × 10 mL). The combined organic layers were washed with brine, dried over Na_2SO_4 and evaporated under vacuum. The resulting alcohol **11** was used directly in next step without purification. To a stirred solution of **11** (991 mg, 4.65 mmol) in 30 mL CH_2Cl_2 at −5 °C was added PBr$_3$ (1 M in dichloromethane, 9.31 mmol) and the reaction was stirred for 12 h at room temperature. The reaction mixture was then poured in ice water followed by extraction with DCM (3 × 15 mL). The combined organic layers were washed with brine, dried over Na_2SO_4, and evaporated under vacuum. Flash column chromatography of the obtained residue on silica gel furnished 1,3,5-tris(1-bromoethyl-1-*d*)benzene (**12**) as colorless oil (75% yield). R_f = 0.68 (1% EtOAc in hexane); ^1H NMR (400 MHz, CDCl$_3$): δ 7.41 (s, 3H), 2.04 (s, 9H).

4.8.2. 1,3,5-Tris(ethyl-1,1-*d*2)benzene (13)

To a stirred solution of compound **12** (1.4 g, 3.5 mmol) in anhydrous tetrahydrofuran (25 mL) was added LiAlD$_4$ (880 mg, 21 mmol) at −20 °C. The temperature was slowly increased to room temperature, and the reaction mixture was then refluxed for 24 h. Upon completion of the reaction, 10 mL ice-cold water was added dropwise to the reaction mixture on an ice-batch. The products were extracted with ether (2 × 50 mL). The organic phase was washed with water (3 × 50 mL), dried with anhydrous Na_2SO_4, and concentrated by evaporation. Flash chromatography purification on silica gel furnished 1,3,5-tris(ethyl-1,1-*d*2)benzene (**13**) as a colorless liquid (88 mg, 15% yield). Purity: 99% by GC. R_f = 0.88 (1% EtOAc in hexane). ^1H NMR (400 MHz, CDCl$_3$): δ 6.98 (s, 3H), 1.22 (s, 9H); ^{13}C NMR (100 MHz, CDCl$_3$): δ 144.2, 124.8, 28.5–27.9, 15.9. GC–MS (m/z): 168 (M$^+$), 153 (M−CH$_3$), 137 (M−CH$_3$CD$_2$).

4.8.3. 2,4,6-Tris(ethyl-1,1-*d*2)benzenesulfonyl azide (D-2)

To a stirred solution of compound **13** (88 mg, 0.56 mmol) in anhydrous CHCl$_3$ (1 mL) at 0 °C under inert atmosphere was added ClSO$_3$H (2.35 mmol) over 5 min. The reaction was stirred until completion of reaction as monitored by TLC. The reaction mixture was then poured into ice-cold water and extracted with dichloro-

methane (3 × 5 mL). The combined organic layers were washed with brine, dried over Na_2SO_4, and evaporated under reduced pressure to yield 2,4,6-tris(ethyl-1,1-*d*2)benzenesulfonyl chloride (**14**) as colorless oil (98% yield), which was carried out to the next step without further purification. To a stirred solution of this compound (**14**) (136 mg, 0.51 mmol) in acetone/water (1:1) (3 mL) at 0 °C was added NaN$_3$ (66 mg, 1.03 mmol) and left stirred at room temperature. After the reaction reached completion (∼45 min), the reaction mixture was concentrated under reduced pressure, followed by extraction with dichloromethane (3 × 10 mL). The combined organic layers were washed with brine, dried over Na_2SO_4 and evaporated under reduced pressure. The residue was purified by flash chromatography on silica gel yielding 2,4,6-tris(ethyl-1,1-*d*2)benzenesulfonyl azide (**D-2**) in quantitative yield as a colorless oil yield. R_f = 0.61 (5% EtOAc in hexane). ^1H NMR (400 MHz, CDCl$_3$): δ 7.06 (s, 2H), 1.27 (s, 6H), 1.24 (s, 3H); ^{13}C NMR (100 MHz, CDCl$_3$): δ 150.6, 146.3, 132.3, 129.6, 28.2–27.3, 16.6, 14.6. LC–MS (ESI) calculated for $C_{12}H_{11}D_6N_3NaO_2S$ [M+Na]$^+$ m/z: 297.3, Observed: 297.2.

Supplementary data

Supplementary data associated with this article can be found, in the online version, at http://dx.doi.org/10.1016/j.bmc.2014.05.015.

References and notes

1. Davies, H. M. L.; Manning, J. R. *Nature* **2008**, *451*, 417.
2. Muller, P.; Fruit, C. *Chem. Rev.* **2003**, *103*, 2905.
3. Collet, F.; Dodd, R. H.; Dauban, P. *Chem. Commun.* **2009**, 5061.
4. Espino, C. G.; Du Bois, J. *Angew. Chem., Int. Ed.* **2001**, *40*, 598.
5. Fiori, K. W.; Fleming, J. J.; Du Bois, J. *Angew. Chem., Int. Ed.* **2004**, *43*, 4349.
6. Liang, C.; Collet, F.; Robert-Peillard, F.; Muller, P.; Dodd, R. H.; Dauban, P. *J. Am. Chem. Soc.* **2008**, *130*, 343.
7. Sun, K.; Sachwani, R.; Richert, K. J.; Driver, T. G. *Org. Lett.* **2009**, *11*, 3598.
8. Ichinose, M.; Suematsu, H.; Yasutomi, Y.; Nishioka, Y.; Uchida, T.; Katsuki, T. *Angew. Chem., Int. Ed.* **2011**, *50*, 9884.
9. Milczek, E.; Boudet, N.; Blakey, S. *Angew. Chem., Int. Ed.* **2008**, *47*, 6825.
10. Cui, Y.; He, C. *Angew. Chem., Int. Ed.* **2004**, *43*, 4210.
11. Yan, S. Y.; Wang, Y.; Shu, Y. J.; Liu, H. H.; Zhou, X. G. *J. Mol. Catal. A: Chem.* **2006**, *248*, 148.
12. Paradine, S. M.; White, M. C. *J. Am. Chem. Soc.* **2012**, *134*, 2036.
13. Breslow, R.; Gellman, S. H. *J. Chem. Soc., Chem. Comm.* **1982**, *24*, 1400.
14. Au, S. M.; Huang, J. S.; Yu, W. Y.; Fung, W. H.; Che, C. M. *J. Am. Chem. Soc.* **1999**, *121*, 9120.
15. Cenini, S.; Gallo, E.; Penoni, A.; Ragaini, F.; Tollari, S. *Chem. Commun.* **2000**, 2265.
16. Yu, X. Q.; Huang, J. S.; Zhou, X. G.; Che, C. M. *Org. Lett.* **2000**, *2*, 2233.
17. Ruppel, J. V.; Kamble, R. M.; Zhang, X. P. *Org. Lett.* **2007**, *9*, 4889.
18. Lu, H.; Jiang, H.; Wojtas, L.; Zhang, X. P. *Angew. Chem., Int. Ed.* **2010**, *49*, 10192.
19. Singh, R.; Bordeaux, M.; Fasan, R. *ACS Catal.* **2014**, *4*, 546.
20. McIntosh, J. A.; Coelho, P. S.; Farwell, C. C.; Wang, Z. J.; Lewis, J. C.; Brown, T. R.; Arnold, F. H. *Angew. Chem., Int. Ed.* **2013**, *52*, 9309.
21. Fita, I.; Rossmann, M. G. *Proc. Natl. Acad. Sci. U.S.A.* **1985**, *82*, 1604.
22. Berglund, G. I.; Carlsson, G. H.; Smith, A. T.; Szoke, H.; Henriksen, A.; Hajdu, J. *Nature* **2002**, *417*, 463.
23. Yang, F.; Phillips, G. N., Jr. *J. Mol. Biol.* **1996**, *256*, 762.
24. Vojtechovsky, J.; Chu, K.; Berendzen, J.; Sweet, R. M.; Schlichting, I. *Biophys. J.* **1999**, *77*, 2153.
25. Finzel, B. C.; Poulos, T. L.; Kraut, J. *J. Biol. Chem.* **1984**, *259*, 13027.
26. Gray, H. B.; Stiefel, E. I.; Valentine, J. S.; Bertini, I. *Biol. Inorg. Chem., Univ. Sci.* **2006**. 6th ed.
27. Adachi, S.; Nagano, S.; Ishimori, K.; Watanabe, Y.; Morishima, I.; Egawa, T.; Kitagawa, T.; Makino, R. *Biochemistry* **1993**, *32*, 241.

28. Yamada, H.; Makino, R.; Yamazaki, I. *Arch. Biochem. Biophys.* **1975**, *169*, 344.
29. Battistuzzi, G.; Bellei, M.; Casella, L.; Bortolotti, C. A.; Roncone, R.; Monzani, E.; Sola, M. *J. Biol. Inorg. Chem.* **2007**, *12*, 951.
30. Lin, L.; Pinker, R. J.; Phillips, G. N.; Kallenbach, N. R. *Protein Sci.* **1994**, *3*, 1430.
31. Yonetani, T.; Asakura, T. *J. Biol. Chem.* **1969**, *244*, 4580.
32. Yonetani, T.; Yamamoto, H.; Woodrow, G. V., 3rd *J. Biol. Chem.* **1974**, *249*, 682.
33. Heinecke, J. L.; Yi, J.; Pereira, J. C.; Richter-Addo, G. B.; Ford, P. C. *J. Inorg. Biochem.* **2012**, *107*, 47.
34. Lelyveld, V. S.; Brustad, E.; Arnold, F. H.; Jasanoff, A. *J. Am. Chem. Soc.* **2011**, *133*, 649.
35. Varnado, C. L.; Goodwin, D. C. *Protein Expression Purif.* **2004**, *35*, 76.
36. Dumon-Seignovert, L.; Cariot, G.; Vuillard, L. *Protein Expression Purif.* **2004**, *37*, 203.
37. Fiori, K. W.; Espino, C. G.; Brodsky, B. H.; Du Bois, J. *Tetrahedron* **2009**, *65*, 3042.
38. Woodward, J. J.; Martin, N. I.; Marletta, M. A. *Nat. Methods* **2007**, *4*, 43.
39. Park, H. S.; Hohn, M. J.; Umehara, T.; Guo, L. T.; Osborne, E. M.; Benner, J.; Noren, C. J.; Rinehart, J.; Soll, D. *Science* **2011**, *333*, 1151.
40. Redaelli, C.; Monzani, E.; Santagostini, L.; Casella, L.; Sanangelantoni, A. M.; Pierattelli, R.; Banci, L. *ChemBioChem* **2002**, *3*, 226.